Technical Report

# Formability of similar and dissimilar friction stir welded AA 5182-H111 and AA 6016-T4 tailored blanks

C. Leitão [a], B. Emílio [b], B.M. Chaparro [a,c], D.M. Rodrigues [a,*]

[a] CEMUC, Department of Mechanical Engineering, University of Coimbra, Coimbra, Portugal
[b] DEM, IST, University of Lisbon, Lisbon, Portugal
[c] ESTA, Polytechnic Institute of Tomar, Abrantes, Portugal

## ARTICLE INFO

## ABSTRACT

The formability of similar and dissimilar tailor welded blanks (TWBs), obtained by friction stir welding of 1 mm thick plates of AA 5182-H111 and AA 6016-T4 aluminium alloys, was analysed by deep drawing cylindrical cups. The metallurgical and mechanical characterization in tension of the welds was already published elsewhere [Leitao C, Leal RM, Rodrigues DM, Loureiro A, Vilaça P. Tensile behaviour of similar and dissimilar AA5182-H111 and AA6016-T4 thin friction stir welds. Mater Design 2009;30:101–8]. In order to understand the formability behaviour of the TWBs, the base materials anisotropy was studied by performing tensile tests at several angles with the rolling direction. Two different types of round TWBs, with 180 and 200 mm diameter, were used in the deep drawing tests. From current study it was possible to conclude that the formability of the TWBs is strongly influenced by the type of mismatch in mechanical properties, between the welds and the base materials, and also, by the initial size of the blanks. Rupture of the cups only occurred under the presence of weld defects, which confirms the good plastic behaviour of the friction stir welds both in overmatch and undermatch conditions.

## 1. Introduction

Friction stir welding (FSW) can be an important joining technology for the automotive industry. In fact, this welding process is probably the solution to overcome some of the usual problems associated with the fusion welding of aluminium alloys, but is also an important step in nowadays environmental concerns by the possibility of reducing material waste and avoiding radiation and harmful gas emissions usually associated with the fusion welding processes. However, to apply FSW in one of the leading areas of the automotive industry, such as the production of tailor welded blanks (TWB), important information is still required both on the metallurgical and mechanical characterization of the welds and on the formability of the friction stir welded tailored blanks.

To the authors knowledge, the few works published addressing the formability of aluminium friction stir welded tailored blanks were conducted on 2 and 3 mm thick plates. Sato et al. [2] and Hirata et al. [3,4] examined the relationship between the microstructure of the FS welds and its formability for the 5052 and 5083 aluminium alloys, respectively. Miles et al. [5,6] analysed the formability of similar and dissimilar TWBs obtained by FSW of the AA 5754-O, AA 5182-O and AA 6022-T4 aluminium alloys. The formability of the TWBs was evaluated using transverse tensile tests and the LDH (Limit Dome Height) and OSU (Ohio State University) tests.

Recently, Silva et al. [7] published a paper focused on the single point incremental forming (SPIF) of AA1050-H111 aluminium tailor welded blanks produced by FSW. The TWBs were made in similar and dissimilar combinations of sheets with 1.5 and 2 mm thickness and its formability was evaluated by means of benchmark tests carried out on truncated conical and pyramidal shapes. The TWBs formability results were compared with the results of similar tests performed on base material blanks. This work showed that the combination of SPIF with tailor welded blanks produced by FSW can be promising in the manufacture of complex sheet metal parts with high depths.

In present study, the formability of similar and dissimilar TWBs, obtained by FSW of 1 mm thick plates of AA 5182-H111 and AA 6016-T4 aluminium alloys, was analysed by deep drawing cylindrical cups. Due to its remarkably different welding and forming behaviour and its potential industrial interest, the joining of AA5xxx and AA6xxx alloys in dissimilar TWBs, 2 and 3 mm thick, was already investigated by several authors. Giera et al. [8] performed a statistical investigation and determined FSW process parameter windows for joining AA 5182 and AA 6016 sheets, 1 mm thick, in similar TWBs. Leitao et al. [1] and Loureiro et al. [9] also analysed the microstructure, hardness distribution and tensile properties of FS welds in these materials. Some of these results will be used in present text to explain the formability results.

* Corresponding author. Tel.: +351 239 790 700; fax: +351 239 790 701.
*E-mail address:* dulce.rodrigues@dem.uc.pt (D.M. Rodrigues).

## 2. The base materials

The base materials used in this work are two aluminium alloys currently used in the automotive industry: AA 5182-H111 and AA 6016-T4. The nominal chemical composition of these alloys is shown in Table 1. The AA5182 aluminium alloy sheets, supplied annealed and slightly cold worked (H111), are characterised by a high content on Mg, exhibiting Portevin-Le Châtelier effect under plastic deformation, which induces an uneven surface of the plates after deformation, restricting the application of this alloy to the production of inner automobile panels. However, due to its excellent formability, especially during deep drawing with a high amount of stretch forming, this material is ideally suited for intricate inner critical applications. The second aluminium alloy, the AA 6016, is a solution alloy heat-treated and naturally aged to a stable condition (T4). This aluminium alloy, that presents stable formability characteristics in the T4 condition, is usually used for car skin sheet applications.

Previously to the formability tests, a mechanical characterization of the base materials was performed, that included monotonic tensile tests at different angles ($\alpha$) to the rolling direction (RD), namely, 0°, 15°, 30°, 45°, 60°, 75° and 90°. These tests were performed by using a universal tensile test machine and longitudinal and transverse strain gages for strain data acquisition. In order to account for the anisotropic properties of the materials, seven uniaxial tensile yield stresses ($\sigma_\alpha$) and r-values ($r_\alpha$) were determined. In Fig. 1, the normalized yield stresses ($\sigma_\alpha/\sigma_0$) and the r-values, registered from the tensile tests, are plotted as a function of the angle with the rolling direction. The r-ratios are calculated from the fitting of the width ($\varepsilon_w$) versus thickness ($\varepsilon_t$) plastic deformation curves from 0.2% to 20% of equivalent plastic deformation. As it can be seen in the figure, the A6016 alloy displays stronger anisotropy in r than the A5182 alloy. Both alloys exhibit small anisotropy in yield stress.

## 3. Characterization of the welds

The welds were produced in 1 mm thick plates of both base materials by using a steel tool with a scrolled shoulder (Fig. 2). The threaded probe was 3 mm in diameter and 0.9 mm long and the scrolled shoulder had 14 mm in diameter. A conventional milling machine provided with steel clamping and backing devices, to firmly fix the plates, was used to execute the welds. Welds were done with tool control position by moving the tool at 320 mm/min travelling speed and 1120 rpm rotational speed. Similar (A5182–A5182 and A6016–A6016) and dissimilar (A5182–A6016) TWB's were made by welding 125 × 250 × 1 mm base material plates parallel to the rolling direction. For the dissimilar TWBs, the A5182 plates were always positioned at the advancing side of the welding tool. In the next, the similar TWBs from the A5182 and A6016 base materials will be labelled as S55 and S66, respectively, and the dissimilar TWBs as D56.

The surface appearance of the weld crowns is shown in Fig. 3a (S55), Fig. 3b (S66) and Fig. 3c (D56). As it can be seen in the figure, no flash was produced during the weld process but the weld surfaces are deeply rough. Small depth striations are observable for
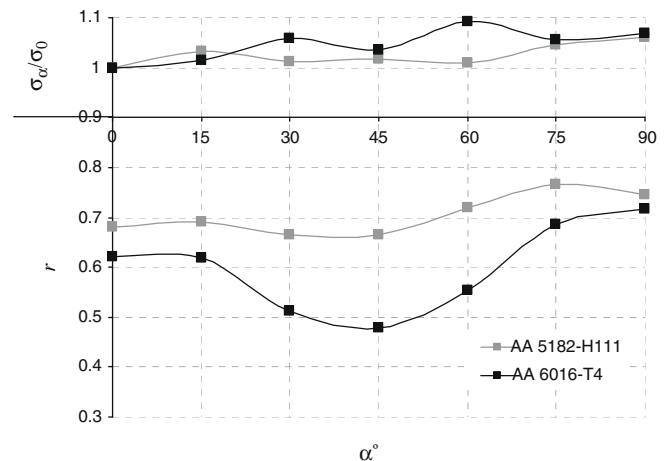


**Fig. 1.** Variation of the normalized yield stress and anisotropy coefficients (r) in the sheet plane.

the S66 and D56 welds. Thickness reduction in the stirred zone was almost inexistent for all the welds. In the formability tests, the TWBs were positioned in order to guarantee that the smooth weld root surface is oriented to the exterior surface of the cups.

After several weeks of natural aging at room temperature, the heterogeneity in mechanical properties across the welds was evaluated by performing several micro-hardness measurements transversely to the weld direction, at 0.75 mm from the weld root. The loads used in the micro-hardness tests were: 50 g for the AA5182 base material and S55 similar welds, 100 g for the AA6016 base material and S66 similar welds and 75 g for the D56 dissimilar welds.

Tensile specimens were also machined from the friction stir welded plates longitudinal and transverse to the welding direction. The results of the micro-hardness and tensile tests, for the base materials and welds, are shown in Fig. 4 and Table 2, respectively. The yield stress values ($R_{ys}$) indicated in Table 2 for the base materials correspond to the $\sigma_0$ yield stresses registered in the 0° tensile tests. In Fig. 4, the mean hardness values of the base materials are represented by straight dashed lines identified as AA 5182-H111 and AA 6016-T4. Results of a metallographic analysis of these welds, which enabled to understand the microstructural evolution across the welds and its relation with the mechanical properties, can be found in Leitao et al. [1].

According to the results presented in Fig. 4 and Table 2, it is possible to conclude that the welds S55 had an increase in hardness around 20% relative to the A5182 base material. This hardness change is accompanied by a significant increase in yield stress of the weld material (S55_L in Table 2). The ductility of the S55 welds, both longitudinally and transversely to the weld direction, is very similar to that of the A5182 base material. On the other hand, the S66 welds displayed a drop of 15% in hardness and around 20% in tensile strength (S66_L in Table 2) relative to the base material A6016. This strength drop is followed by an important loss in ductility for the transverse samples, due to the localization of the plastic flow in the weakest weld line. Finally, the D56 dissimilar welds exhibit a hardness variation consistent with the complex microstructure evolution registered across the TMAZ of these welds as reported in [1,10]. Contrarily to the S66 similar welds, no significant decrease in hardness was observed in the A6016 side of the D56 welds (retreating side, Fig. 4). In the A5182 side of the D56 welds (advancing side, Fig. 4) it was registered an increase in hardness of the same magnitude of that measured for the S55 welds. In accordance with this hardness evolution, the yield stress of both longitudinal (D56_L) and transverse (D56_T) tensile samples of

**Table 1**
Nominal chemical composition of the base materials (wt%).

| Alloy | Si | Fe | Cu | Mn | Mg | Cr | Zn | Ti |
|---|---|---|---|---|---|---|---|---|
| AA5182-H111 | <0.2 | <0.35 | <0.15 | 0.2–0.5 | 4.0–5.0 | <0.1 | <0.25 | <0.1 |
| AA6016-T4 | 1.0–1.5 | <0.5 | <0.2 | <0.2 | 0.25–0.6 | <0.1 | <0.2 | <0.15 |

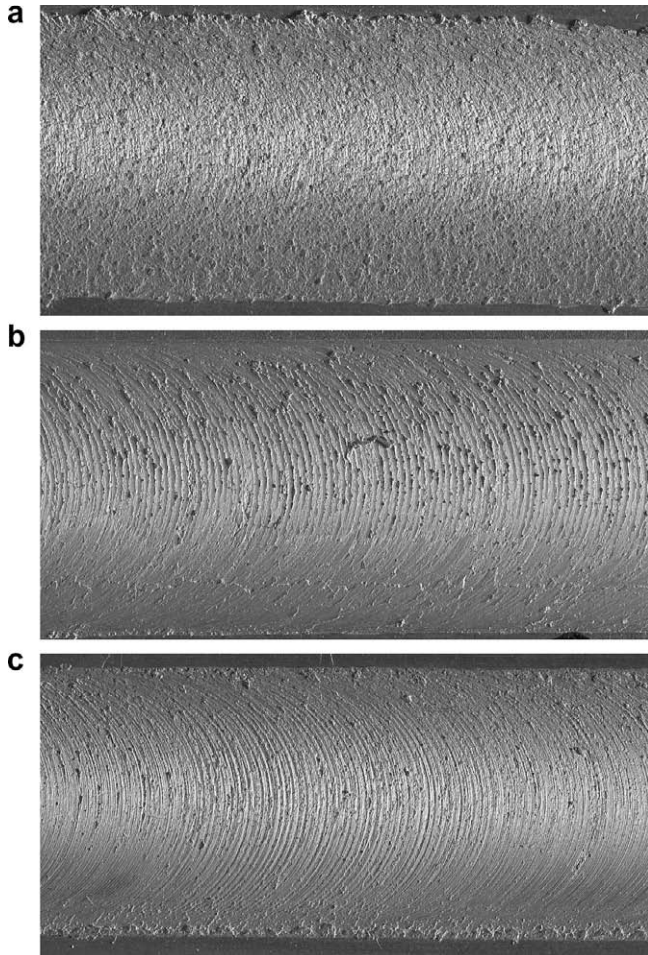**Fig. 2.** FSW tool.



**Fig. 3.** Weld crown appearance for the S55 (a), S66 (b) and D56 (c) welds.
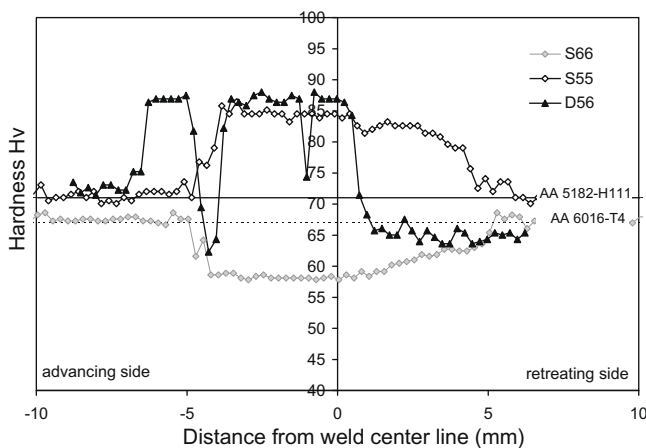


**Fig. 4.** Hardness profiles across the S55, S66 and D56 welds.

**Table 2**
Tensile test results overview.

|  |  | $e$ (%) | $R_{ys}$ (MPa) | $R_m$ (MPa) |
|---|---|---|---|---|
|  | A5182 | 24 | 108 | 275 |
|  | A6016 | 24 | 104 | 226 |
| Longitudinal sample | S55_L | 21 | 204 | 296 |
| Transverse sample | S55_T | 22 | 118 | 278 |
| Longitudinal sample | S66_L | 19 | 134 | 185 |
| Transverse sample | S66_T | 7 | 108 | 185 |
| Longitudinal sample | D56_L | 8 | 151 | 222 |
| Transverse sample | D56_T | 8 | 116 | 202 |

$e$ – Elongation at fracture; $R_{ys}$ – yield strength; $R_m$ – tensile strength 0.3.

the dissimilar welds is superior to both base materials yield stresses and the tensile strength is 90% of that of the weakest base material, the A 6016 alloy. However, due to the previously mentioned microstructural heterogeneity characteristic of these welds, the ductility of the D56 samples seriously decreases relative to the base materials. No substantial changes were observed in the microstructure and mechanical properties on the HAZ relative to the base materials, neither in the advancing nor in the retreating sides of the welds [1].

## 4. Formability tests

### 4.1. Experimental procedure

The formability of the TWBs was evaluated by stamping cylindrical cups with a special tool developed to be operated in a standard universal tensile test machine. This testing device comprises a 100 mm punch, a 110 mm diameter die and a blank-holder. Fig. 5a shows a sketch of the tool and Fig. 5b and c show pictures of the stamping device before and after testing, respectively.

The tool was built using AISI P20 tool steel, for the tool parts that will be in contact with the blank, and AISI 1045 steel, for all other structural components. The average surface roughness is 0.21, 0.35 and 0.32 μm for the punch, die and blank-holder, respectively. To apply and maintain the force in the blank-holder, 10 calibrated springs were used. One of these springs was equipped with a 10 kN force sensor in order to verify if the blank-holder force remained stable during the tests. The stamping operation was always performed on lubricated blanks. The lubricant used was the deep drawing QUAKER N6130 oil. It was applied 1.4 g/m² of oil per blank face using a pre-impregnated paper weighted before and after the application. In this work, cylindrical cups 60 mm deep were obtained from 180 mm (D18) and 200 mm (D20) round blanks of both base materials and TWBs. The TWBs had the weld located at the center line, as shown in Fig. 6. The punch speed was 100 mm/min and several blank-holder forces ($F_{bh}$) were tested, namely, 8 kN for the D20 blanks and 8, 16, 20 and 32 kN for the D18 blanks.

### 4.2. Formability results

#### 4.2.1. Similar tailor welded blanks

The punch force–displacement ($F$–$D$) curves registered during the deep drawing test of the D20 and D18 blanks of both base materials and similar TWBs (S55 and S66), with $F_{bh}$ = 8 kN, are shown in Fig. 7. As it can be observed from the figure, independently of the blank materials, the punch force curves have higher values for the D20 blanks than for the D18. However, after the maximum punch force value is reached, the rate of punch force decrease is higher for the D18 blanks. This is because the amount of material under the blank-holder is smaller for the D18 blanks than for the D20 blanks, making easier the flow of the blank material
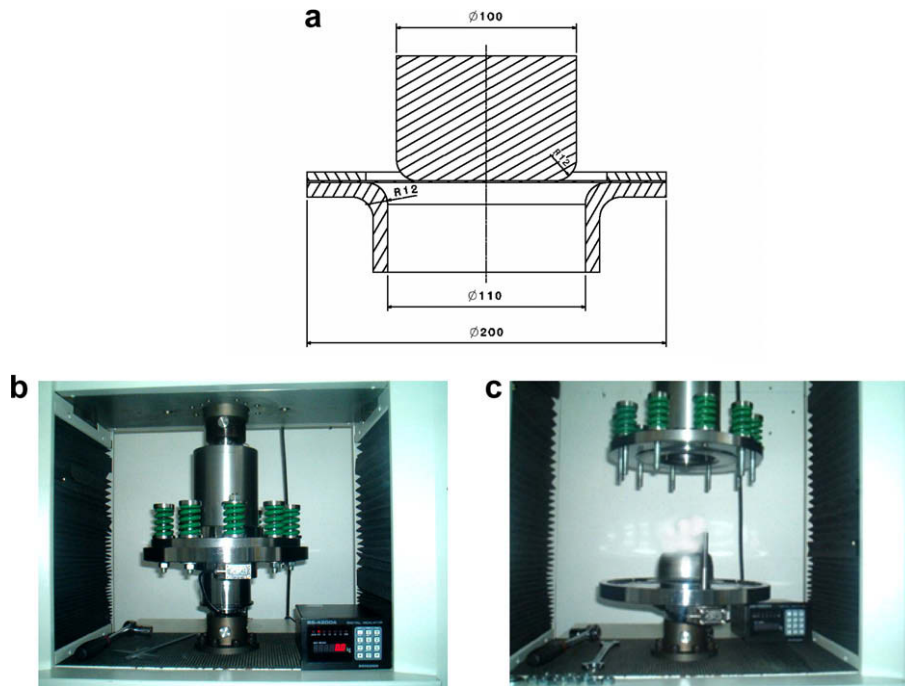
**Fig. 5.** Sketch of the stamping tool (a) and images of the initial (b) and final (c) stages of the stamping operation.



**Fig. 6.** Tailor welded blanks.

into the die. It is also important to observe that, for both types of blanks (D18 and D20), the drawing force evolution is very similar for the A5182 and S55 blanks and for the A6016 and S66 blanks. However, for the D20 blanks, the maximum punch force for the S55 blanks is slightly higher than for the A5182 blanks. This behaviour can be related with the overmatch mechanical properties of the S55 welds.
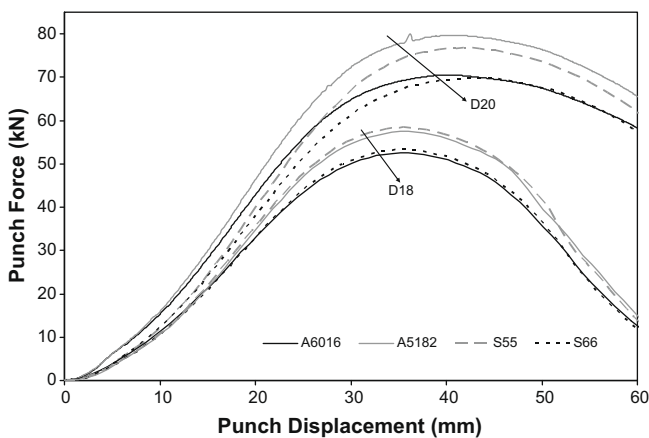


**Fig. 7.** Punch force evolution for the D18 and D20 base materials (A5182 and A6016) and similar TWBs (S66 and S55).

In Figs. 8 and 9 are shown pictures of the base materials and TWB cups obtained from the D20 and D18 blanks, respectively. These cups correspond to the drawing tests of Fig. 7 ($F_{bh}$ = 8 kN). As it can be observed in the figure, with both types of blanks it was possible to achieve TWB cups without rupture, which confirms de good formability behaviour of the welds already depicted from the F–D curves. It is also possible to observe in Fig. 8b and d that the cups, obtained from the A6016 and S66 blanks, display ears resulting from the planar anisotropy of the A6016 base material already depicted in Fig. 1. Earing is not observable for the cups obtained from the A5182 blanks, since this material is much less anisotropic.

In Fig. 10 are shown pictures of the outer surface of a S66-D20 cup and a cut plane from a S55-D18 cup. In these pictures it is possible to observe that, after deep drawing, the weld roots have no defects (Fig. 10.a) and have very smooth appearance with no thickness mismatch near to the weld line (Fig. 10b). Concerning the global appearance of the cups, for the D20 blanks (Fig. 8), it is possible to observe that all the cups have regular shape with no visible defects. Despite some wrinkling tendency can be observed for all the D20 cups, the flange surface is very smooth. It is also important to observe that, unless by the presence of the weld, the base material and TWB cups have the same appearance.

However, reducing the diameter of the blanks to 180 mm (Fig. 9), the final shape of the TWB cups is very different from that of the cups of the respective base materials. In fact, for the S55 blanks, a deep material bending over the weld was formed at the flange area as can be observed in Fig. 9c and in the magnification of this area presented in Fig. 11a. For the A6016 and S66 cups (Fig. 9b and d), despite the anisotropy of the base material, it is possible to observe that earing was almost restricted to the portion of material near the weld line of the S66 cup. In fact, since the S66 weld material is softer than the base material, it undergoes stronger plastic deformation under the same blank-holder load. In Fig. 11b it is possible to observe a magnification of this area where the intense plastic deformation of the weld is obvious. Several blank-holder forces (16, 20 and 32 kN) were tested in order to
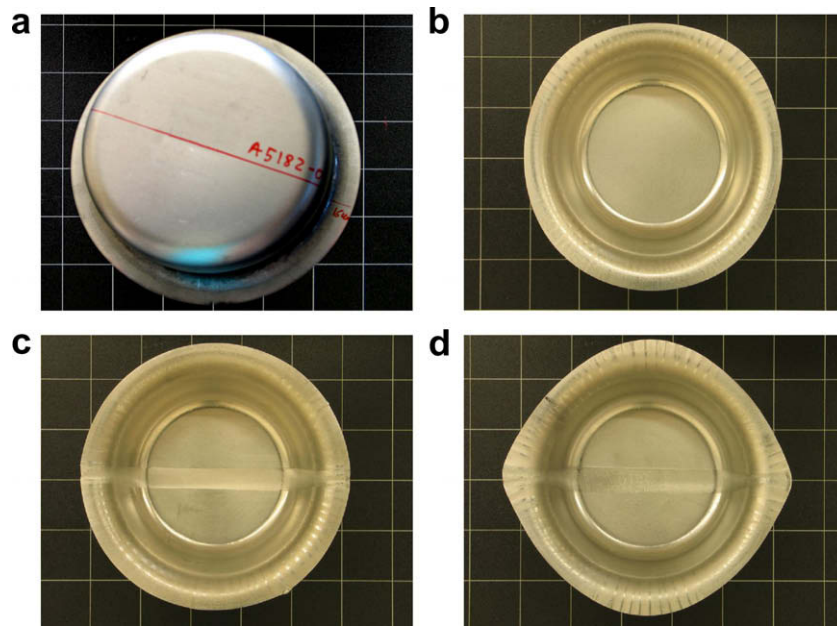
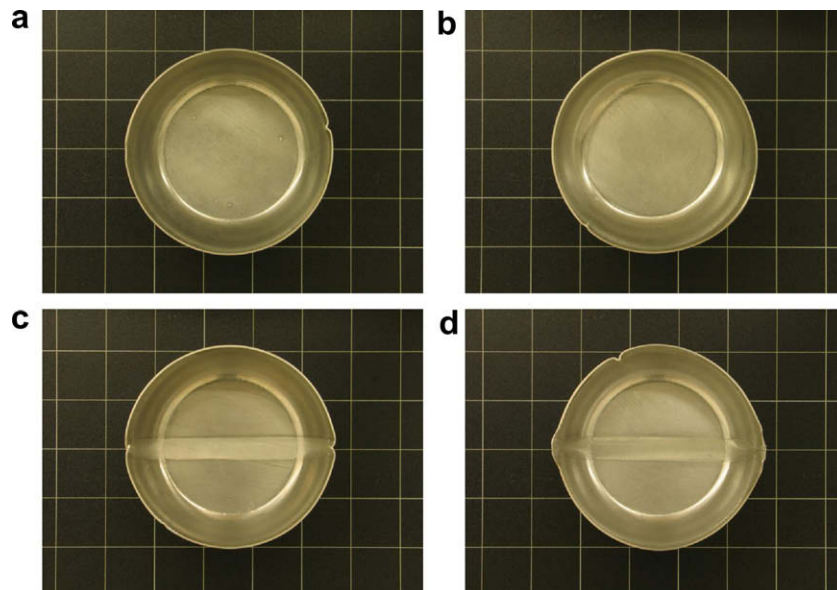**Fig. 8.** Cups from A5182 (a), A 61016 (b), S55 (c) and S66 (d) D20 blanks.



**Fig. 9.** Cups from A5182 (a), A 61016 (b), S55 (c) and S66 (d) D18 blanks.

try to reduce the stamping defect in the S55-D18 cups. However, it was observed that the cups geometry remained similar to that obtained with $F_{bh}$ = 8 kN. The S66 blanks were also tested under the same drawing conditions of the S55 blanks, and again, the obtained cups had the same characteristics of that obtained under 8 kN blank-holder force.

*4.2.2. Dissimilar tailor welded blanks*

Previously to the formability tests, visual inspection revealed the presence of small flaws (Fig. 12) at the root face of some of the dissimilar welds. These flaws resulted from the imprecision in tool control positioning when performing the welds with the conventional milling machine. Since these defects were present in all the D20 dissimilar TWBs, it was not possible to obtain cups without rupture from these blanks. The same problem occurred

with the D18 dissimilar TWBs that were drawn with $F_{bh}$ = 8 kN. However, it was possible to obtain cups without rupture from the D18 dissimilar TWBs (the welds in these TWBs were defect free) drawn with 16, 20 and 32 kN blank-holder forces (Fig. 13).

As it can be observed from Fig. 13, despite the heterogeneity in mechanical behaviour between the two base materials, after deep drawing, the weld line remained straight and aligned at the middle line of all the cups. The dissimilar TWB cups also have very similar characteristics, independently of the blank-holder force used in the tests. Comparing the shape of the dissimilar cups with that of the similar ones, it is possible to conclude that the D56 blanks conjugate the forming characteristics of the S55 and S66 blanks. In fact, at the cup flange, near the weld line, it is possible to see strong bending, in the A5182 side of the TWB, and earing at the A6016 side of the TWB. In Fig. 11c is shown a magnification of this

**Fig. 10.** Magnifications of the weld roots of the S66-D20 (a) and S55-D18 (b) cups.



**Fig. 12.** Weld root flaw in a dissimilar D56 weld.

area in a D56 cup (16 kN), which enables to compare its similarities with both magnifications of the same area of the S55 (Fig. 11a, 8 kN) and S66 (Fig. 11b, 8 kN) cups. However, it is important to enhance that the bending defect at the A5182 side of the dissimilar cups becomes less pronounced when the blank-holder force is increased from 16 to 32 kN (Fig. 13a and c).

In Fig. 14 are shown the $F$–$D$ curves obtained for the different types of D18 welded blanks (S66, D56 and S55), for the tests perfo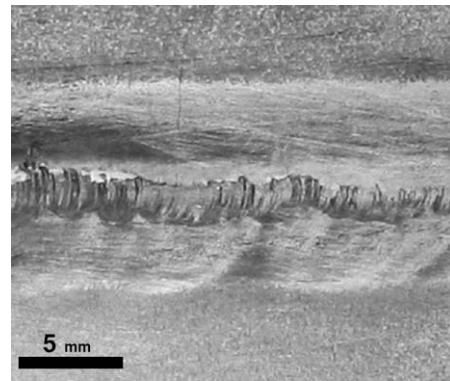rmed with $F_{bh}$ = 32 kN. In this graph it is possible to observe that the curve of the D56 blank follows between the curves of the two similar TWBs, but has similar shape of that of the S66 blank. The shape of the S55 curve is also different from that of the curve registered for the S55 blanks in the 8 kN blank-holder force tests (Fig. 7). In fact, in the graph of Fig. 14, an abrupt force decrease is visible in the curve of the S55 blank, which suggests that the blank was released by the blank-holder during the stamping operation. For the S66 and D56 blanks, it is not possible to observe such an abrupt decrease in punch force. This is due to the formation of hears in the vicinity of the weld during the stamping operation, which makes that some portion of weld material remain trapped by the blank-holder until the end of stamping operation.
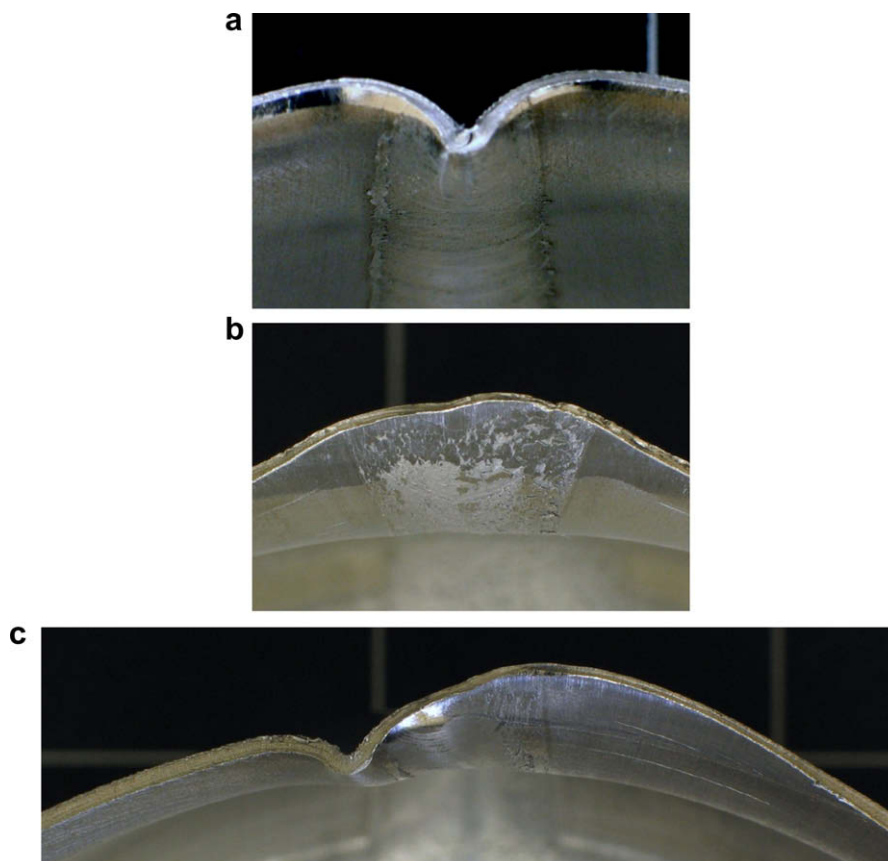


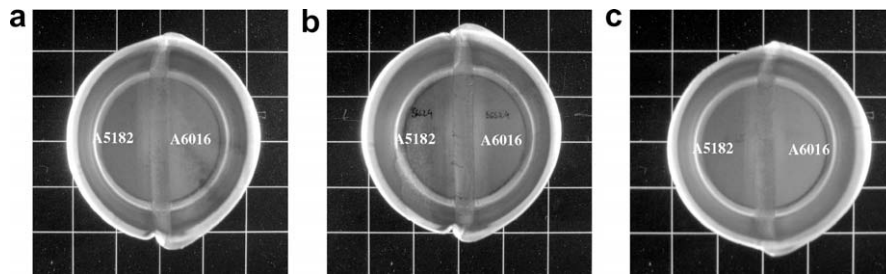**Fig. 11.** Magnifications of the cups flange near to the S55 (a), S66 (b) and D56 (c) welds.

**Fig. 13.** Cups from D56-D18 blanks drawn with 16 kN (a), 20 kN (b) and 32 kN (c) blank-holder forces.

In the graph of Fig. 15 are summarised the maximum punch forces attained during deep drawing of the S55, S66 and D56 blanks under the different blank-holder forces considered in this study. As it can be concluded from the graph, the maximum punch forces registered for the S55 blanks increase, with increasing blank-holder force. This is a regular behaviour since, under increasing blank-holder force, the normal pressure between the sheet flange and the blank-holder increases, increasing the friction and making more difficult the flow of the material into the die, and thus, increasing the punch force. However, for the S66 and D56 blanks, for blank-holder forces higher than 8 kN, the maximum punch force attained in the tests remain almost constant. This may be indicative that necking occurred in the blanks, which makes that the necessary increase in the punch force due to the increasing blank-holder forces, is compensated by the force decrease due to plastic strain localization in the blank material.

Since necking in plastically deformed parts occurs by localized thinning, some of the cups were cut and the thickness variation along the cup walls was measured. The results obtained for the S55 and S66 cups, formed with 32 kN blank-holder force, are shown in Fig. 16. As it can be seen in the figure, minimum thicknesses values were registered at the cups bottom radius and vertical side walls and thickening at the flange area. It is well known that blank thickening near the top of the cup sections occurs due to the friction at the die/blank interface and due to the circumferential forces. Comparing the thickness profile near the cups bottom, where thinning occurs, it is possible to conclude that it is different for the two types of blanks. In fact, meanwhile for the S55 cup the thickness reduction occurs gradually along the cup radius, for the S66 cup, lower thickness values were registered in a very localized region (see numbers in bold in both figures), indicating the beginning of necking in this area.
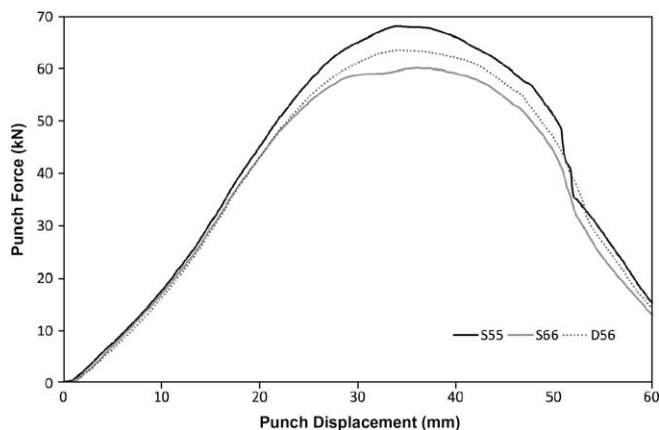


**Fig. 15.** Maximum punch force in the drawing tests of the D18 blanks ($F_{bh}$ = 8, 16, 20 and 32 kN).



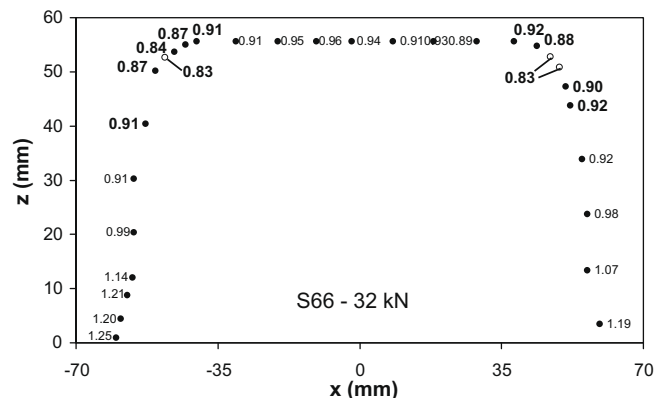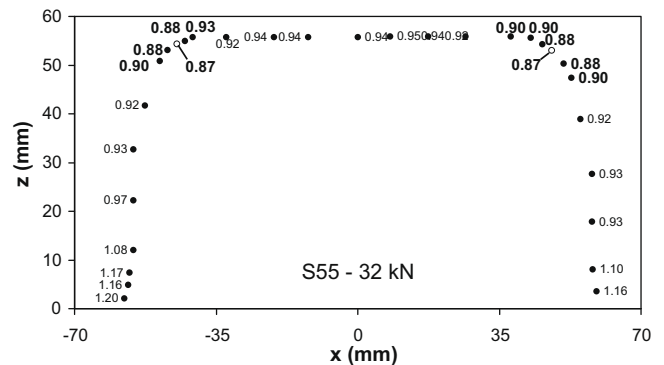**Fig. 14.** Punch force evolution for the D18 TWBs ($F_{bh}$ = 32 kN).



**Fig. 16.** Thickness variation along the cup walls measured in the S66 and S55 cups.

## 5. Conclusions

The formability of similar and dissimilar TWBs, obtained by friction stir welding of 1 mm thick plates of AA 5182-H111 and AA 6016-T4 aluminium alloys, was analysed by deep drawing cylindrical cups. From this study it was possible to conclude that the formability of the TWBs is influenced by the mismatch in mechanical properties between the weld and the base materials, and also, by the initial size of the blanks. In fact, when using TWBs with 200 mm diameter, it was possible to obtain non-defective cups for both the overmatched (S55 welds) and undermatched (S66 welds) similar welded blanks. The final geometry of the TWBs cups was very similar to that of the correspondent base material cups (A5182 and A6016) which confirm the excellent plastic behaviour of the friction stir welds. Reducing the size of the blanks to 180 mm diameter, the formability behaviour of the overmatched and undermatched similar welded blanks becomes drastically different. For the S55 blanks (overmatched welds) strong bending over the weld was observed at the flange of the cups. This defect remained even increasing the blank-holder force from 8 to 32 kN, which proves the necessity of using larger blanks for improving the formability of these blanks. For the undermatched TWBs (S66 blanks), the only defect observed was the formation of small ears, at the flange of the cups, resulting from stronger plastic deformation of the undermatched weld material. These small defects, which remain with the same characteristics, even increasing the blank-holder forces used in the tests, can be easily eliminated by machining the TWBs after forming.

Finally, for the dissimilar TWBs, it was found that the presence of small defects at the weld root of the dissimilar welds induced rupture of some of the blanks during the formability tests, namely, the blanks with 200 mm diameter and the blanks with 180 mm in diameter tested with 8 kN blank-holder force. However, it is was possible to drawn without rupture 180 mm diameter blanks under higher blank-holder forces (16, 20 and 32 kN) which proves that the rupture resulted exclusively from the presence of the defects and the dissimilar TWBs have good formability behaviour. In fact, it was observed that the dissimilar TWBs tested under the same conditions of the similar ones, conjugated the forming characteristics of the S55 and S66 blanks, displaying bending, in the A5182 side of the TWB, and earing, at the A6016 side of the TWB. These defects were localized at the cup flange, near the weld line, and presumably could be avoided by increasing the blanks diameter. The increase in blank-holder force from 16 to 32 kN also mitigate the bending effect at the A5182 side of the dissimilar TWBs. However, such high values of blank-holder force are very close to the rupture forming limit of the A6016 base material. In fact, necking evidences were detected for the S66 and D56 blanks, by analysing the maximum punch force evolution under increasing blank-holder forces and by measuring the evolution of the thickness along the cup walls.

## Acknowledgements

## References

[1] Leitao C, Leal RM, Rodrigues DM, Loureiro A, Vilaça P. Tensile behaviour of similar and dissimilar AA5182-H111 and AA6016-T4 thin friction stir welds. Mater Design 2009;30:101–8.

[2] Sato YS, Sugiura Y, Shoji Y, Park SHC, Kokawa H, Ikeda K. Post-weld formability of friction stir welded Al alloy 5052. Mater Sci Eng A 2004;369(1–2): 138–43.

[3] Hirata T, Oguri T, Hagino H, Tanaka T, Wook CS, Tsujikawa M, et al. Formability of friction stir welded and arc welded 5083 aluminum alloy sheets. Key Eng Mater 2007;340–341:1473–8.

[4] Hirata T, Oguri T, Hagino H, Tanaka T, Chung SW, Takigawa Y, et al. Influence of friction stir welding parameters on grain size and formability in 5083 aluminum alloy. Mater Sci Eng A 2007;456:344–9.

[5] Miles MP, Decker BJ, Nelson TW. Formability and strength of friction-stir-welded aluminum sheets. Metall Mater Trans A 2004;35:3461–8.

[6] Miles MP, Melton DW, Nelson TW. Formability of friction-stir-welded dissimilar-aluminum-alloy sheets. Metall Mater Trans A 2005;36:3335–42.

[7] Silva MB, Skjoedt M, Vilaça P, Bay N, Martins PAF. Single point incremental forming of tailored blanks produced by friction stir welding. J Mater Process Tech 2008;209(2):811–20.

[8] Giera A, Merklein M, Geiger M. Statistical investigations on friction stir welded aluminum tailored blanks for a robust process window. Adv Mater Res 2005;6–8:599–606.

[9] Loureiro A, Leal RM, Leitão C, Rodrigues DM, Vilaça P. Friction stir welding of automotive aluminium alloys. Weld World 2007;51:433–40.

[10] Leal RM, Leitão C, Loureiro A, Rodrigues DM, Vilaça P. Material flow in heterogeneous friction stir welding of thin aluminium sheets: effect of shoulder geometry. Mater Sci Eng A 2008;498(1–2):384–91.